

**Michael T. Lippert, Kentaroh Takagaki, Weifeng Xu, Xiaoying Huang and Jian-Young Wu**

*J Neurophysiol* 98:502-512, 2007. First published May 9, 2007; doi:10.1152/jn.01169.2006

**You might find this additional information useful...**

---

This article cites 46 articles, 26 of which you can access free at:

<http://jn.physiology.org/cgi/content/full/98/1/502#BIBL>

Updated information and services including high-resolution figures, can be found at:

<http://jn.physiology.org/cgi/content/full/98/1/502>

Additional material and information about *Journal of Neurophysiology* can be found at:

<http://www.the-aps.org/publications/jn>

---

This information is current as of July 12, 2007 .

# Methods for Voltage-Sensitive Dye Imaging of Rat Cortical Activity With High Signal-to-Noise Ratio

Michael T. Lippert,\* Kentaroh Takagaki,\* Weifeng Xu, Xiaoying Huang, and Jian-Young Wu

Department of Physiology and Biophysics, Georgetown University Medical Center, Washington, DC

Submitted 1 November 2006; accepted in final form 8 May 2007

**Lippert MT, Takagaki K, Xu W, Huang X, Wu J-Y.** Methods for voltage-sensitive dye imaging of rat cortical activity with high signal-to-noise ratio. *J Neurophysiol* 98: 502–512, 2007. First published May 9, 2007; doi:10.1152/jn.01169.2006. We describe methods to achieve high sensitivity in voltage-sensitive dye (VSD) imaging from rat barrel and visual cortices in vivo with the use of a blue dye RH1691 and a high dynamic range imaging device (photodiode array). With an improved staining protocol and an off-line procedure to remove pulsation artifact, the sensitivity of VSD recording is comparable with that of local field potential recording from the same location. With this sensitivity, one can record from ~500 individual detectors, each covering an area of cortical tissue 160  $\mu\text{m}$  in diameter (total imaging field ~4 mm in diameter) and a temporal resolution of 1,600 frames/s, without multiple-trial averaging. We can record 80–100 trials of intermittent 10-s trials from each imaging field before the VSD signal reduces to one half of its initial amplitude because of bleaching and wash-out. Taken together, the methods described in this report provide a useful tool for visualizing evoked and spontaneous waves from rodent cortex.

## INTRODUCTION

Voltage-sensitive dye (VSD) imaging, an optical method of measuring transmembrane potential, has developed into a powerful tool for studying brain activity since pioneering work was published >30 yr ago (Cohen et al. 1968; Tasaki et al. 1968). VSD molecules bind to the membranes of excitable cells and report changes in membrane potential by shifting their absorbance or fluorescence spectra. Although the optical signal of VSD has excellent linearity with membrane potential (within a range of approximately  $\pm 300$  mV) and very fast response time ( $<1$   $\mu\text{s}$ ) (Ross et al. 1977), the optical signal is small. Fractional changes in absorption or fluorescence are only  $\sim 10^{-5}$ – $10^{-2}$  of the resting absorption/fluorescence intensity per 100 mV of membrane potential change. In biological experiments, such small signals are quite vulnerable to noise and artifacts. For imaging in vitro preparations such as brain slices and cultured cells, noise and artifact can be controlled well and the sensitivity of VSD imaging rivals that of local field potential recordings (Jin et al. 2002). In contrast, imaging the mammalian cortex in vivo is more difficult because hemoglobin absorbance causes a large pulsation artifact. This artifact can sometimes exceed evoked cortical signals by an order of magnitude (Grinvald and Hildesheim 2004; London et al. 1989; Ma et al. 2004; Shoham et al. 1999).

New “blue” dyes, developed by Amiram Grinvald’s group (Shoham et al. 1999), have brought a great advance for in vivo

imaging of mammalian cortex. The excitation wavelength of blue dyes has minimal overlap with the absorption of hemoglobin and hence has minimal pulsation artifact (Shoham et al. 1999). Although research reports using blue dyes have been published in recent years (Ferezou et al. 2006; Petersen et al. 2003a,b; Slovín et al. 2002), many technical issues have not been examined. These include methods for reaching a high sensitivity, optimum staining, the reduction of residual pulsation artifact, and limitations in recording time caused by bleaching and photo-toxicity. In this study, we show methods to achieve high signal-to-noise ratio recordings using VSD, with sensitivity as good as that of local field potential recording. This sensitivity allows for recording of spontaneous and evoked activity in single trials without spatial or temporal averaging. We will also discuss methodological issues such as elimination of residual pulsation artifacts, the total possible duration of optical recording experiments, and how deep in the cortex the dye can reach, when stained transdurally.

## METHODS

### *Surgery*

Sprague-Dawley and Long Evans rats (250–400 g) were used in the experiments. Surgical procedures were approved by Georgetown University Animal Care and Use Committee following National Institutes of Health guidelines.

Animals were pretreated with atropine sulfate (40  $\mu\text{g}/\text{kg}$ , ip) ~30 min before anesthetic induction to reduce mucus secretion. The animals were induced with 2–3% isoflurane in air, and tracheostomy was performed. A 16-G over-the-needle catheter was inserted into the trachea, and animals were ventilated by a small animal respirator (Harvard Apparatus) with isoflurane in room air. Respiration rate (60–100/min) and volume (2–4 ml) were adjusted such that inspiratory pressure was ~5 cmH<sub>2</sub>O and the end-tidal carbon dioxide (ETCO<sub>2</sub>) was maintained at ~26–28 mmHg, with a calibrating multigas monitor (BCI 9100). Next, the animal was placed in a stereotaxic frame with a regulated heating pad. As soon as the animal was secure, isoflurane was reduced to 1.5–2% for surgery and during recordings unless specified otherwise. In some experiments, the anesthesia level was lowered, and xylazine was used to augment the level of anesthesia. The animals were closely monitored to ensure sufficient anesthetic plane, using heartbeat response to tail-pinch. Because the depth of isoflurane anesthesia is sensitive to hypothermia (Regan and Eger 1967), care was taken to ensure normothermia throughout recording. Lac-

\* M. T. Lippert and K. Takagaki contributed equally to this work.

Address for reprint requests and other correspondence: J.-Y. Wu, The Research Building, WP26, 3970 Reservoir Rd., NW, Washington, DC 20057 (E-mail: wuj@georgetown.edu).

The costs of publication of this article were defrayed in part by the payment of page charges. The article must therefore be hereby marked “advertisement” in accordance with 18 U.S.C. Section 1734 solely to indicate this fact.

tated Ringer solution was periodically infused ( $\sim 2.5$  ml/kg/h, sc) to compensate for urination and insensitive fluid loss, and bland ophthalmic ointment was applied periodically to the eyes to prevent corneal desiccation.

The cranial surface was cleaned thoroughly of soft tissue, and a thin layer of surgical adhesive (Vetbond, 3M) was applied to prevent dye leakage during staining. Next, a cranial window ( $\sim 5$  mm diam) was drilled on the left hemisphere over visual cortex (bregma,  $-4$  to  $-9$  mm; lateral,  $1-6$  mm) or barrel field (bregma,  $-0$  to  $-5$  mm; lateral,  $2-7$  mm). Bone was carefully separated from the dura, which was left intact. Leaving dura intact significantly reduces the movement artifact during optical recording (London et al. 1989). Care was taken to avoid irritation of the cortex by heat or pressure during this procedure. The drill tip was immersed in artificial cerebrospinal fluid (ACSF) during drilling to diffuse heat from the drilling. Nontraumatic craniotomy was found to be important for better staining. Irritated brain can appear reddish (because of increased blood flow), or CSF pressure can increase the potential subdural space, which leads to poor staining. In some experiments, dexamethasone sulfate ( $1$  mg/kg, ip) was given  $24$  h before the experiment to reduce inflammatory response of the dura.

### Staining

VSD RH1691 (Optical Imaging) was dissolved at  $2$  mg/ml in ACSF solution, and staining was done through the intact dura mater.

To increase the dural permeability to the dye, we dried the dura before staining. The surface of the dura mater was washed with ACSF, after which the fluid was removed thoroughly by suction. The dura mater was allowed to dry completely for  $3-4$  min, with gentle air flow, until the tissue became very transparent and "glassy." This glassy appearance is essential for good staining. Occasionally, longer drying ( $\leq 15$  min) was needed. The drying procedure did not alter local field potential profiles of the cortex.

A temporary staining chamber was constructed around the craniotomy with a thin layer of silicone valve grease. We used  $\sim 200$   $\mu$ l of dye solution ( $\sim 2$  mg/ml of RH1691) to stain an area  $5$  mm in diameter. During staining, the dye solution was continuously circulated by a custom-made perfusion pump (London et al. 1989). The pump had a battery-powered gear motor that gently pressed the rubber nipple of a Pasteur pipette once every few seconds. The tip of this pipette was placed in the staining solution and performed a gentle, back-and-forth circulation of a small amount of dye ( $\sim 100$   $\mu$ l). Such circulation was necessary because CSF slowly exudes from the dura and dilutes the dye concentration locally at the dye/dura interface. Staining lasted for  $90$  min, followed by washing with dye-free ACSF for  $>15$  min.

### Physical stabilization of the cortex

By leaving the dura mater intact, we greatly increased the physical stability of the brain, and a sealed chamber was not necessary. In some preparations, we applied high viscosity silicon oil (60,000 centistokes, Sigma DMPS-60M) on top of the dura to further dampen cortical pulsation. This silicon oil was replaced every  $30$  min to  $1$  h, because exuded CSF would accumulate underneath and hinder the dampening effect.

Firm fixation within the stereotaxic frame and maintenance of proper body posture, hydration, and  $ETCO_2$  can minimize the movement of the skull caused by heartbeat and respiration. In some experiments, we paralyzed the animal with pancuronium bromide ( $1$  mg/kg, im) and paused ventilation during optical recording to completely eliminate the respiratory movement. When ventilation was paused during recording, longer intertrial intervals ( $1-2$  min) were given.

### Imaging apparatus

The cortex was imaged by a  $\times 5$  microscope with a field of view  $\sim 4$  mm in diameter (Fig. 1), following the designs of Kleinfeld (Kleinfeld and Delaney 1996) and Cohen (Precht et al. 1997). The microscope was assembled from commercial video camera lens (Navitar,  $25$  mm F0.95) and provides high numerical aperture to effectively collect fluorescent emission from the cortex. The microscope has a numerical aperture of  $0.45$ , which gathers  $\sim 100$  times more light than an ordinary  $\times 4$  microscope objective.

A halogen tungsten filament lamp ( $12$  V,  $100$  W, Zeiss) was used for illumination. This low-cost lamp is a standard component for upright microscopes and offers stable light with low noise. The light was filtered with a  $630 \pm 15$ -nm interference filter (Chroma Technology) and reflected down onto the cortex through a  $655$ -nm dichroic mirror (Chroma Technology). Köhler illumination was achieved through the microscope (Fig. 1).

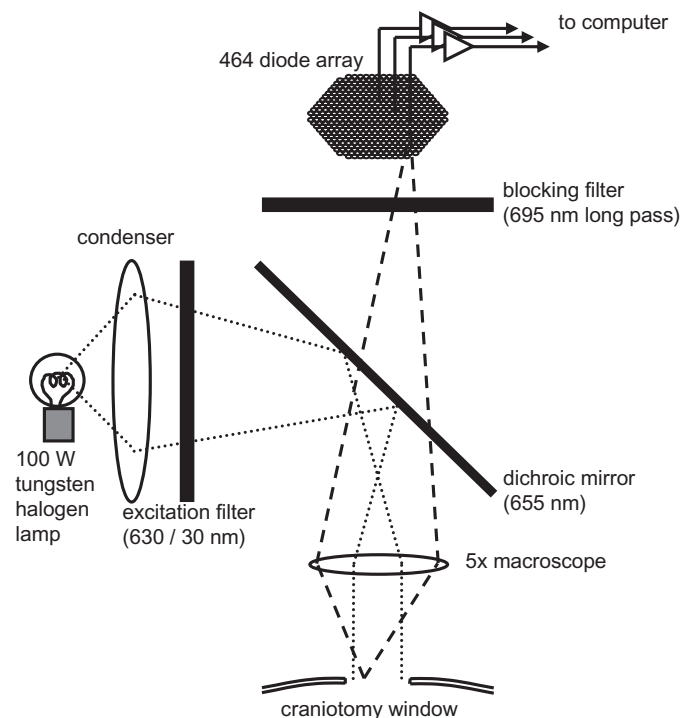


FIG. 1. Schematic drawing of recording apparatus. Light from the tungsten lamp was filtered with a  $630 \pm 15$ -nm band-pass filter and reflected through a  $655$ -nm dichroic mirror for illumination. Filament of lamp is focused onto the back focal plane of the microscope to achieve Köhler illumination. Fluorescent light from the cortex is collected with the microscope, passed through the  $695$ -nm long-pass filter, and forms a real image onto the aperture of diode array. Field of view on the cortex is  $\sim 4$  mm in diameter. Numerical aperture of the microscope is  $\sim 0.45$ , with optical magnification of  $\times 5$  and working distance of  $\sim 20$  mm.

The fluorescence of the dye ( $\sim 700$  nm, Optical Imaging) from the stained cortex was collected through the microscope, filtered through a 695-nm long-pass filter (RG-695, Edmund Scientific), and projected onto the fiber optic aperture of a 464-channel photodiode array (WuTech Instruments). Each channel (detector) of the array received light from a cortical area of  $\sim 160$   $\mu\text{m}$  in diameter. The photocurrent from each channel was individually amplified through a two-stage amplifier (Wu and Cohen 1993). The first stage was an  $I$ - $V$  converter of 50 V/ $\mu\text{A}$  (50-Mohm transimpedance). The fluorescent resting light intensity (RLI) of the stained cortex was about 1 V (20 nA of photo current) at the output of the  $I$ - $V$  converter. The output of the  $I$ - $V$  converter was high-pass filtered at 0.1 or 1.4 Hz to remove the DC component of the light or resting fluorescent light (RLI). The signal was fed into the second amplifier and amplified 500 times. The second stage amplifier only amplifies the differential component of the light and is therefore not saturated by the large RLI. An optical signal of typical sensory-evoked cortical activity was  $\sim 10^{-3}$  of the RLI or  $\sim 500$  mV (peak-to-peak) at the output of the second stage amplifier. This signal was low-pass filtered at 400 Hz and digitized at 1.6 kHz by an A/D converter card (MicroStar DAP-4000) on a PC. Because the RLI is subtracted before the second stage amplifier, the full 12-bit range of the A/D converter is available to digitize the optical signal. The effective dynamic range can reach  $\sim 19$  bits (see DISCUSSION). The apparatus was mounted on a high-performance isolation stage (Minus K Technology) to remove floor vibrations.

### Stimuli

For visual stimulation, we used a flash from a white LED, positioned in front of the contralateral eye. The stimulus lasted for 10 ms and covered  $\sim 40^\circ$  of the visual field of the animal. The light path was shielded to avoid contamination of the stimulation light into the optical recordings. For whisker stimulation, we used a 200-ms ramp-and-hold deflection in the anterior direction. The stimulator consisted of a galvanometer with a small loop on the needle tip, holding the whisker at 10 mm from the base, and provided rapid deflections of 3 mm ( $\sim 15^\circ$ ).

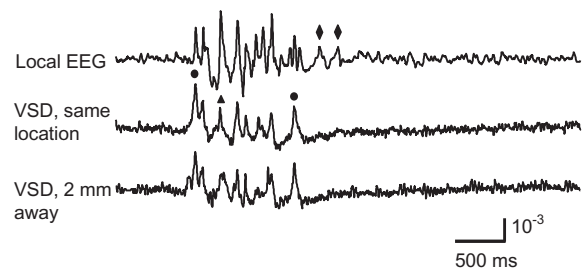
### Local field potential recording

Electrodes were placed on the edge of the optical recording field to record the epidural local field potential. Figure 2 uses a tungsten microelectrode; Fig. 4 uses a silver ball electrode. The signal was amplified 1,000 times using a custom-made amplifier with frequency range of 1–100 Hz. Local field potential was digitized concurrently with optical channels, along with ECG and driving voltage of the stimuli. The ECG was used to remove pulsation artifacts off-line.

### Subtraction of brain pulsation artifact

Although the blue dyes have greatly reduced the artifact caused by hemoglobin absorption (Shoham et al. 1999), movement artifact from brain pulsation is still a major contributor to recording noise. Because pulsation artifact is time locked to the ECG, it can be largely subtracted from each individual trial to observe single trials of VSD activity (Arieli et al. 1995). We used an off-line algorithm for this

### A Spontaneous burst (1.5% isoflurane)



### B Spontaneous oscillations (1.1% isoflurane)

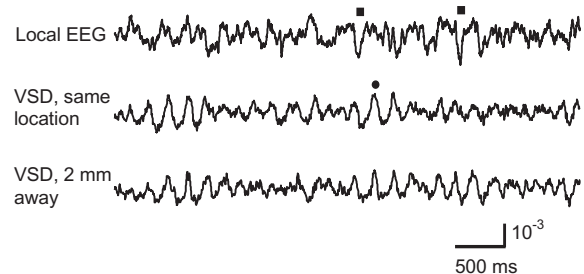


FIG. 2. Sensitivity of voltage-sensitive dye (VSD) recordings. Top 2 traces in each panel are local field potential and VSD recordings from the same location in visual cortex. Another VSD recording (bottom trace in each panel) was 2 mm away from this location. *A*: under 1.5% isoflurane, there are spontaneous spindle-like bursts. Dots mark events in which VSD has higher amplitude than local field potential. Triangles mark events in which local field potential has higher amplitude than VSD. Diamonds mark events seen in local field potential but not in VSD. *B*: recordings from the same animal as in *A*,  $\sim 5$  min later, with isoflurane anesthesia lowered to 1.1%. Most peaks in local field potential are also seen in VSD, but correlation between the 2 signals is lower. Baseline fluctuations cannot be attributed to noise, because analogous recordings had much less fluctuation when anesthesia was elevated (*A*).

subtraction based on previous methods from our laboratory (Ma et al. 2004). In this subtraction algorithm, the peak of QRS waves was obtained from the ECG recorded simultaneously with the imaging trial. An average QRS interval was obtained for each trial, and ECG-triggered averages for each optical detector were obtained spanning three average QRS intervals, 1.5 intervals before the peak and 1.5 intervals after. This “averaged pulsation artifact” was repeatedly concatenated in synchrony with each QRS peak to reconstruct an average trace for each detector. Because the QRS interval varies subtly from heartbeat to heartbeat, simply concatenating the average waveform would produce small jumps at the point of each concatenation. To eliminate such jumps, the concatenation was done with a linear-weighted transition—at QRS peak number  $n$ , the averaged waveform aligned to peak  $n$  was weighted 100%; midway between QRS peak number  $n$  and  $n + 1$ , the waveform aligned to peak  $n$  and  $n + 1$  were weighted at 50% each; at QRS peak number  $n \pm 1$ , the waveform aligned to peak  $n + 1$  is weighted 100%. The resulting concatenated average pulsation artifact for each optical detector was subtracted from the raw data for that detector (Fig. 5). The subtracted signals were analyzed with a fast Fourier transform and show virtually no energy peak at the heartbeat frequency. Matlab code for the procedure is available on request.

### Data analysis

Data were processed in Neuroplex (RedShirt Imaging), Matlab (Mathworks), and Mathematica (Wolfram Research). Scripts are available on request. Pseudocolor movies were generated such that each detector was individually scaled to a linear color scale (Grinvald et al. 1982; Jin et al. 2002).

## RESULTS

### Sensitivity of VSD recordings

With our methods to eliminate pulsation artifact, the sensitivity of VSD recording was comparable to that of local field potential recordings (Fig. 2). In this experiment, we recorded cortical activity by VSD imaging and local field potential simultaneously from the same tissue. Comparing the two signals, we found most of the peaks in the local field potential showed a corresponding event in the VSD trace. Under 1.5% isoflurane anesthesia, infrequent bursts of spontaneous activity occurred on both electrical and optical recordings, and most events within each burst correlated well between local field potential and VSD signals (Fig. 2A). However, local field potential and VSD signals were frequently disproportionate in amplitude. In Fig. 2A, events labeled with dots had higher amplitude in VSD trace compared with that in the local field potential trace, whereas events labeled with triangles had larger amplitude in the local field potential trace compared with that in the VSD trace. Events labeled with diamonds were seen in the local field potential but not in the VSD signals. Adjusting the level of anesthesia allows us to further verify the correlation between local field potential and the VSD signals. When the level of anesthesia was lowered, both VSD and local field potential signals show continuous spontaneous fluctuations (Fig. 2B). The fluctuations in the VSD signals are unlikely to be baseline noise, because the baseline noise is much smaller in the quiescent segments of Fig. 2A, which were obtained from the same location in the same animal. Instead, these fluctuations are likely to be biological signals from local cortical activity, probably sleep-like oscillations or up/down states (Petersen et al. 2003b). Although the correlation between the local field potential and VSD recordings decreased, many events in local field potential were also seen in the VSD traces (exceptions are marked with squares in Fig. 2B). VSD recordings made from two adjacent locations also show good correlation (bottom 2 traces in each panel of Fig. 2), further indicating that the fluctuations on the VSD traces were not noise. Because almost every event in the local field potential can be seen in the VSD recordings, the sensitivity of the VSD measurement is comparable with that of local field potential recordings. However, VSD and local field potential signals have a low overall correlation of  $\sim 0.2$  between 3 and 30 Hz (which includes 90% of the power). This low overall correlation is probably because some local field potential peaks originated from deep cortical layers or subcortical sources.

The correlation between optical traces is much higher, and each peak in the signal appears at many locations (Fig. 2, A and B, bottom traces). This high correlation between optical traces is not from light scattering or optical blurring between channels, because there is a small timing difference between locations, resulting globally in a propagating wave. The spatiotem-

poral pattern of the waves will be further discussed in later sections.

### Staining and the source of the VSD signal

Cortex was stained well after 90 min of staining with RH1691 through the dura mater (Fig. 3A). We sliced the cortex after staining and found that the fluorescence of the dye reached a depth of 500  $\mu\text{m}$  from the cortical surface (Fig. 3A). The fluorescence intensity (Fig. 3A, right) shows that most of the dye fluorescence originates from layers I and II/III; these layers contain  $\sim 70\%$  of the fluorescence signal. The highest intensity is in layer I, which contributes  $\sim 30\%$  to the overall fluorescence. This dye distribution in cortical tissue is similar to that stained with dura removed in rat (Kleinfeld and Delaney 1996; Petersen et al. 2003a) and mice (Ferezou et al. 2006). The distribution of the fluorescence intensity indicates that the VSD signals mostly originate from the layers I–III. In addition, because illumination intensity will decrease with depth while scattering/reabsorption of the dye fluorescence will increase with depth, activity in layer IV and deeper layers have little contribution to the signal. Therefore the VSD signal described here is most likely a combination of synaptic and spiking activity in layer I to II/III. Because the fluorescence of RH1691 is in the near infrared range, visual evaluation from the dural/cortical surface may not reveal the quality of staining. When cortex was visually inspected under room light, only a light blue hue was seen in the tissue (Fig. 3B). However, even with this light visual appearance (as shown in Fig. 3), the stained cortex yields excellent optical signals during imaging (Figs. 4, 5, 7, and 8).

### Comparison of RH1691 and RH795

The pulsation artifact of RH1691 was very small compared with that of RH795 (Fig. 4; Shoham et al. 1999). In this comparison, we used spontaneous epileptiform spikes as the source of VSD signal. Applying bicuculline methiodide to the cortex induces spontaneous epileptiform spikes at a frequency of 1 spike/s (Gutnick et al. 1982). The spikes provide a large VSD signal ( $\sim 10^{-2}$  of resting fluorescent intensity), and the signal is relatively stable from trial to trial and from animal to animal (Ma et al. 2004). We stained with each dye in independent experiments and found both RH1691 and RH795 had similar signal amplitude of epileptiform spikes (Fig. 4). However, the pulsation artifact of RH1691 was much smaller. The amplitude of the pulsation artifact in RH795 was similar to that of the epileptiform spikes, whereas the artifact of RH1691 was only about one seventh of the signal amplitude. This comparison shows a great potential for in vivo imaging using the new blue dyes, as shown in recent reports (Derdikman et al. 2003; Ferezou et al. 2006; Grinvald and Hildesheim 2004; Petersen et al. 2003a,b; Shoham et al. 1999; Spors and Grinvald 2002).

### Removal of residual pulsation artifact

In our experiments, we frequently observe large VSD signals with negligible pulsation artifact (Fig. 5, optical 1). However, residual pulsation artifact can still be large compared with small signals such as spontaneous and sensory-evoked cortical activity. Figure 5 compares residual pulsation artifact at various locations within the visual cortex. At some locations, the

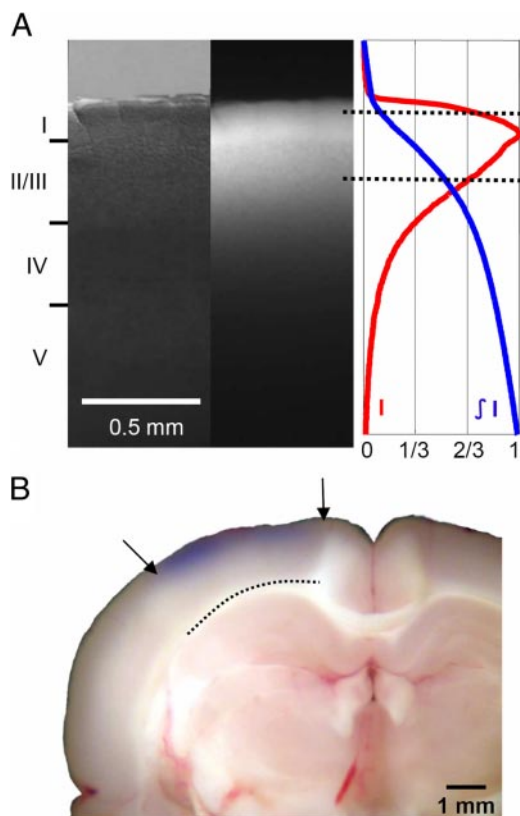


FIG. 3. Staining depth. *A*: *left*: visible light image of the stained cortex. *Middle*: fluorescence image from the same cortical section showing distribution of RH1691 staining. *Right*: fluorescence intensity (red) and integrated fluorescence intensity (blue). Broken lines mark tissue depth with fluorescent intensity higher than two thirds of maximum intensity. *B*: photograph of a stained cortical section. Arrows indicate boundary of cranial window. Broken line indicates border between gray and white matter. Staining of RH1691 can be seen by eye as a light blue hue.

pulsation artifact was almost absent (Fig. 5, optical 1). Other locations had pulsation artifact of varying waveform and polarities (Fig. 5, opticals 2 and 3). These traces suggest that the artifact is mainly contributed by movement because of pulsation, because movement artifact can have either polarity at various locations while the polarity of hemoglobin absorption should be consistent at all cortical locations.

To remove residual pulsation artifact, an off-line subtraction procedure is necessary. The procedure can effectively remove artifact that is time locked with the ECG, regardless of polarity and waveform (Fig. 5). There were  $\sim 50$  heartbeats in each 10-s recording trial; therefore in the averaged artifact trace (see METHODS), signal and noise components that are not correlated to the heartbeat were reduced to  $\sim 1/50$  of their original amplitude, and  $\sim 98\%$  of the artifact can be removed (Fig. 5, bottom traces).

#### Total recording time

In brain slices, the recording time of VSD imaging is mainly limited only by dye bleaching (Jin et al. 2002; Momose-Sato et al. 1999). Using absorption dyes in brain slices, the total optical recording time is  $\sim 1,800$  s before the VSD signal declines to one half of the initial amplitude (Jin et al. 2002). Under in vivo conditions, other factors such as washing out of

the dye by blood circulation may also reduce the total recording time. Therefore the total recording time must be determined empirically.

To determine the feasible total recording time, we measured the decrease of VSD signal (RH1691) under an illumination intensity of  $\sim 1.5 \times 10^{11}$  photo-electrons/mm<sup>2</sup> ms (at this intensity, the sensitivity of VSD imaging is comparable with that of local field potential recordings). We used spontaneous epileptiform spikes induced by bicuculline methiodide as the source of VSD signal. Epileptiform spikes provide a large VSD signal ( $\sim 10^{-2}$ ), and the signal is relatively stable from trial to trial and from animal to animal (Ma et al. 2004). The cortex was illuminated intermittently, with 20 s of light exposure each minute. The amplitude of the VSD signal was plotted along with exposure time in Fig. 6.

Decay of VSD signal did not follow a simple exponential process. Instead, a flat period followed by a declining period was observed. The flat period lasted for 300–800 s of light exposure (Fig. 6A). During this period, no apparent decay in the signals was seen, whereas in some areas, the signal amplitude actually increased. After the flat period, the amplitude of the signal had a steady decline (Fig. 6A). The length of the flat period varies from animal to animal. In one of four animals, the staining was less optimal and the flat period was much shorter (Fig. 6A, stars), suggesting that the flat period is related to the wash-out of the dye from the stained tissue. Because the boundary between flat and declining periods was not clearly distinguishable, we use the “half-time,” i.e., the duration of exposure for the signal to reduce to 50% of its beginning amplitude, as the total recording time. In three animals with

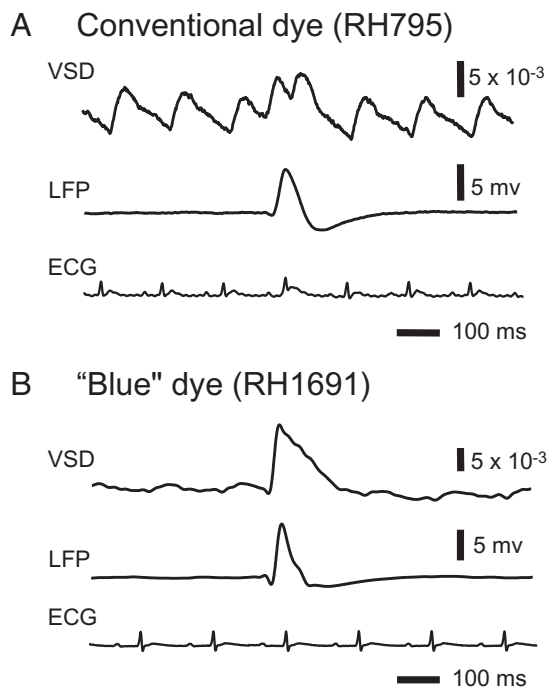


FIG. 4. Comparison of RH795 and RH1691. Recordings from 2 separate animals stained with RH795 and RH1691 (*A* and *B*, respectively). Epileptiform spikes induced by bicuculline had large signals in both VSD and local field potential recordings (top and middle traces on each panel). Pulsation artifact was time locked to the ECG (bottom traces on each panel). VSD signal from RH795-stained cortex had large pulsation artifact, comparable in amplitude with epileptiform spike (*A*), whereas the artifact was much smaller in VSD signal from RH1691-stained cortex.

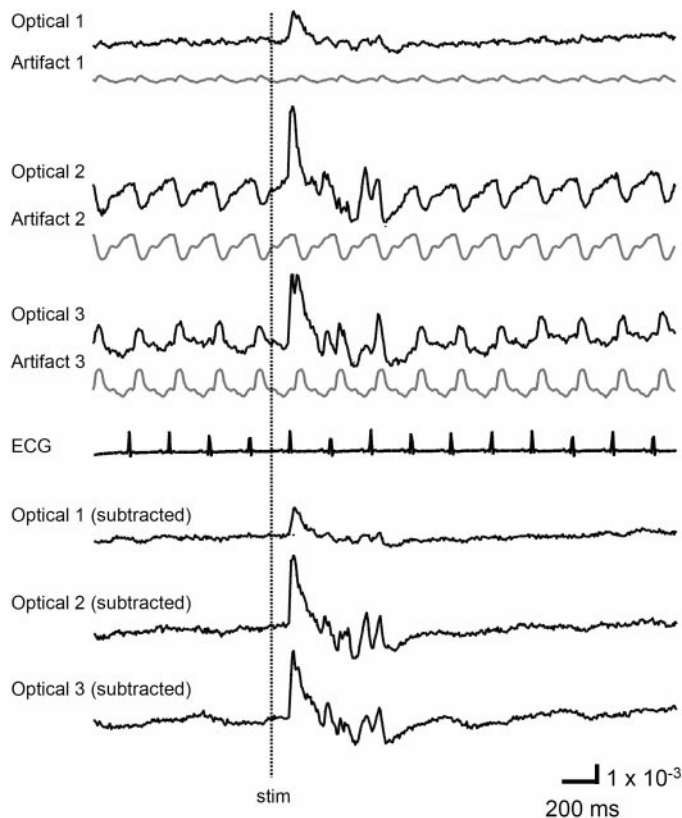


FIG. 5. Pulsation artifact of RH1691. VSD signals from 3 locations of visual cortex are shown (opticals 1–3, black traces on the top). Visually evoked cortical activity was seen at all 3 locations when the contralateral eye was stimulated by a light flash (stim). Gray trace under each raw black trace is pulsation artifact, reconstructed with an ECG-triggered averaging procedure. Note that in 1 location (optical 1), there was virtually no pulsation artifact. Pulsation artifact is time-locked to ECG and contains virtually no components from recorded activity. After subtraction, signals from the 3 locations had similar waveforms and contained almost no artifact (bottom 3 traces).

good staining, the total recording time was 800–1,000 s. This time should allow for 80–100 recording trials of 10 s each, which is sufficient for most experiments.

To further distinguish dye wash-out from light-related amplitude reduction, we shielded part of the cortex from light during a light exposure experiment (Fig. 6B). After the signal in the exposed area transitioned to the declining period, the shield was removed. Signal from the previously shielded area had similar amplitude as that in the flat period. (Fig. 6B, solid dots). However, the signal in the shielded area did not show a flat period; instead, the signal declined at a similar rate as the unshielded regions. This suggests that the flat period was related to the dye wash-out, which only occurred within a certain period after the staining.

Our data indicate that one can collect 800–1,000 s of data before the VSD signal reduced to one half of the initial amplitude. This estimated time was shorter than previous reports (Shoham et al. 1999), probably because we use higher illumination intensity for higher sensitivity (Fig. 7).

### Sensory-evoked activity

We were able to reliably detect sensory-evoked cortical activity in single trials. Signals in Fig. 7 were recorded from

individual detectors (160  $\mu\text{m}$  in diameter) in single trials, showing the ability to achieve a high spatiotemporal resolution. The evoked activity had lower amplitude when evoked at certain phases of spontaneous activity (Fig. 7, A, traces 8 and 10, and B, traces 3 and 6). Variations in evoked cortical activity also occurred in spatial pattern.

### Propagating waves

Both spontaneous and evoked cortical activity manifested as propagating waves (Fig. 8). Sensory evoked waves followed a consistent propagation pattern, initiating from the location of the thalamic afferents and spreading to large areas of the cortex. In barrel cortex, the whisker evoked waves initiated from within the corresponding barrel and propagated to the entire barrel cortex (Fig. 8A, top row), with an overall velocity of  $0.2 \pm 0.1$  m/s ( $n = 6$  animals). In visual cortex, flash evoked waves started from V1 and propagated to other visual areas (Fig. 8B, top row). Visually evoked waves had a similar overall velocity as those in the barrel cortex. Spontaneous events originated from various locations and propagated with larger variations in direction

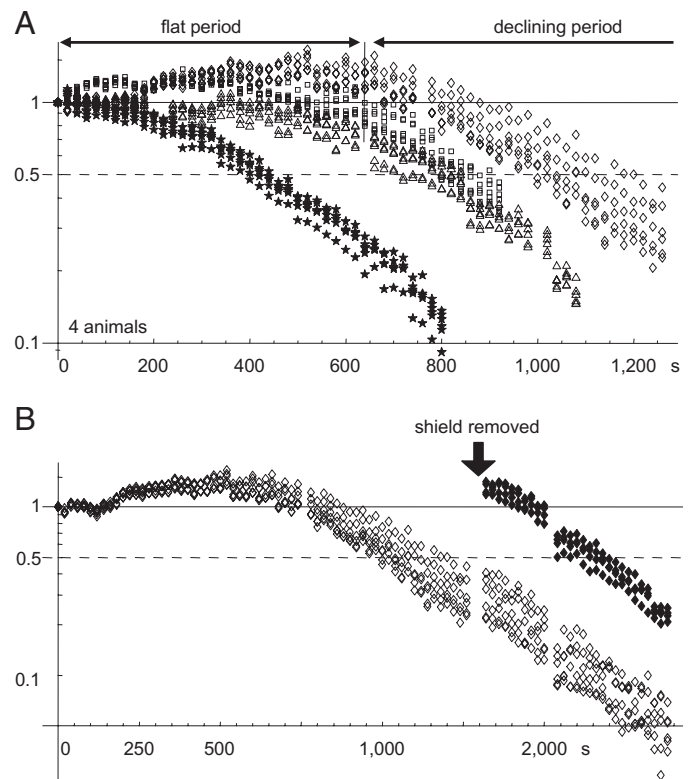
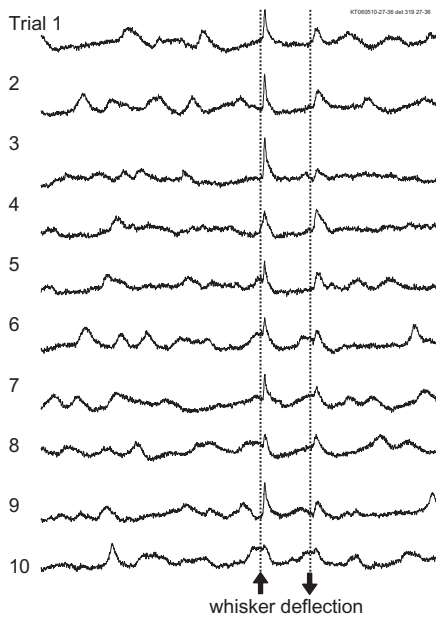
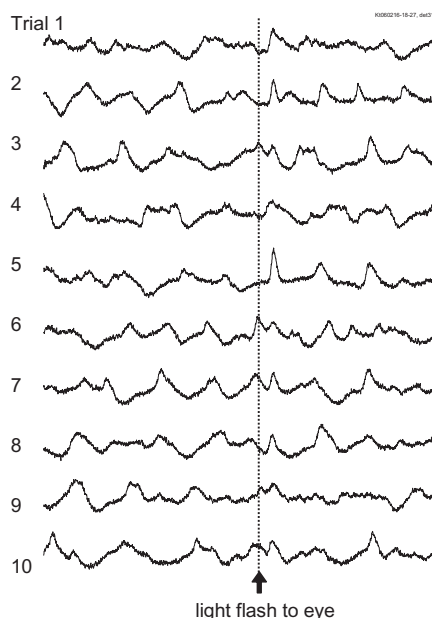


FIG. 6. Total recording time. A: amplitude of VSD signal (bicuculline-induced spikes) is plotted against light exposure time. Data from 4 animals were normalized to amplitude of the 1st recording trial. In 3 animals (diamonds, triangles, squares), signal amplitude remained stable (or slightly increased) for a period (flat period). After the flat period, signal had a higher rate of decline with light exposure (declining period). Note that 1 animal did not have optimum staining, and stable time was much shorter (stars). B: data from another animal, in which part of the cortex was shielded from light exposure. In the shielded area, signal amplitude remained unchanged (solid diamonds), whereas signal in unshielded area declined (empty diamonds), suggesting that signal decline was related to light exposure. Shielded area did not have a flat period after shielding was removed, suggesting that the flat period may be related to dye wash-out.

**A** Barrel cortex



**B** Visual cortex



2x10<sup>-3</sup>  
200 ms

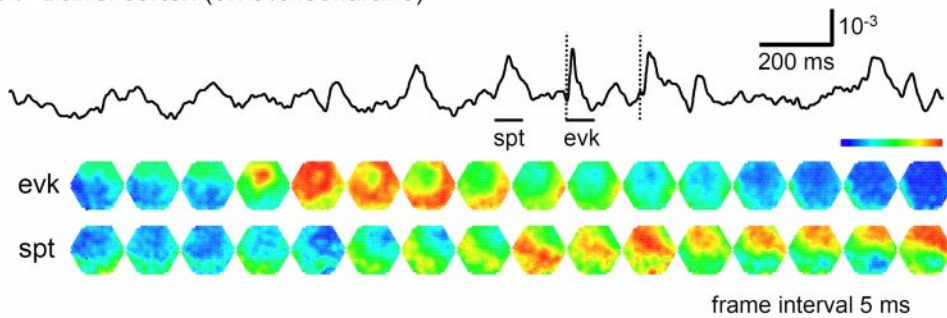
FIG. 7. Sensory-evoked response. *A*: signal from a single detector viewing a cortical area of 160  $\mu\text{m}$  in diameter near principal barrel in the barrel cortex. Ten trials are displayed from 105 trials with identical whisker stimuli. *B*: signal from a single detector viewing a cortical area of 160  $\mu\text{m}$  in diameter in V1 area. Ten trials are displayed from  $\sim 30$  trials recorded with identical light stimuli to the contralateral eye.

and velocity (Fig. 8, *A* and *B*, bottom rows). The spontaneous event in Fig. 8*B* appears as two waves: one propagating from the bottom left to upper right and followed immediately by another wave in the opposite direction. The spontaneous and evoked waves we have observed are consistent with reports from other groups (Derdikman et al. 2003; Petersen et al. 2003b).

*Trial-to-trial variations*

Obtaining data with high signal-to-noise ratio, from hundreds of trials from each animal, allows us to examine trial-to-trial variations of cortical activity evoked by identical sensory stimuli. Large trial-to-trial variations were observed in both visual and barrel cortex (Fig. 7). In the barrel cortex, the

**A** Barrel cortex (0.75% isoflurane)



**B** Visual cortex (2% isoflurane)

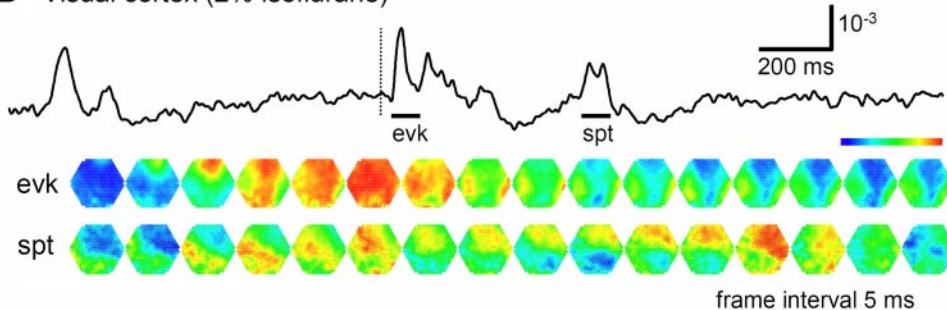


FIG. 8. Propagating waves in barrel and visual cortices. Top traces in *A* and *B* are signals from a single detector in recording field. Bars under each trace mark time of a spontaneous event (spt) and an evoked response (evk) during recording trial. Vertical broken lines mark time of stimulation. Bottom images in each panel are frames showing spatiotemporal patterns of evoked (top row) and spontaneous events (bottom row). Imaging field is  $\sim 4$  mm in diameter. Each image is a 0.625-ms snapshot, with every 8th frame displayed (5-ms frame intervals). Bars under top trace mark duration of images. *A*: in barrel cortex, evoked response started from principal barrel and spread as a propagating wave to entire imaging field within 15 ms. Spontaneous event started from bottom of the field and propagated as a slow wave across field. *B*: in visual cortex, sensory-evoked wave is slower than that in the barrel cortex. Note that spontaneous wave in visual cortex was initiated from the bottom of the field, propagated upward, and reflected near the top to propagate downward.

evoked wave started from the correspondent whisker barrel in all trials and propagated to the entire barrel field. However, individual trials showed large trial-to-trial variations in signal amplitude (Fig. 7) and propagation pattern (Fig. 9).

Trial-to-trial variations in propagation pattern manifest as anisotropy of propagating pattern and velocity (Fig. 9). In Fig. 9, the propagation pattern of individual trials was compared with that of the multiple trial average. Although all trials show a similar overall spatiotemporal pattern, significant trial-to-trial variations can be seen in individual trials: The onset times for trials 2, 3, and 10 are shorter than the average, whereas in trials 1 and 8, the onset times are longer. In the *bottom row* of Fig. 9, the contour lines of the propagation patterns for trials 5, 6, 8, and 10 are superimposed to compare them with the contours of the average pattern. The contour lines are highly variable, suggesting that the propagation of an evoked wave is highly dynamic. Because spontaneous waves occurred frequently, they may interact with the evoked response and contribute to anisotropic propagation patterns. In trial 5, the evoked activity seemed to merge with a spontaneous event and propagated faster in the direction toward the spontaneous event (Fig. 9).

Overall, the blue dye RH1691 exhibited an excellent signal and low pulsation artifact, allowing the use of a high dynamic range imaging device to achieve sensitivity comparable with that of local field potential recordings. Such ability provides a useful tool to examine spatiotemporal dynamics in the cortex when multitrial averaging is not possible.

DISCUSSION

Imaging of mammalian cortex in vivo has benefited greatly from the blue dyes developed by the Grinvald group (Shoham

et al. 1999), which provides a signal largely devoid of pulsation artifact related to hemoglobin (Fig. 4; Ferezou et al. 2006; Shoham et al. 1999). Therefore the sensitivity of the VSD recording can be greatly enhanced, to the limit of shot noise—which is the quantal unevenness in the light flux. Using a photodiode array can take full advantage of the blue dyes to achieve high-sensitivity recordings, limited only by shot noise. The main point of this report is to show that the sensitivity of VSD recordings under these conditions can be comparable with that of local field potential recordings (Fig. 2) when photodiode arrays are used in combination with blue dyes.

Saturation intensity and dynamic range of the imaging device

Visualizing spatiotemporal dynamics in single trials requires higher sensitivity than mapping active areas in the cortex. To visualize VSD signals of  $10^{-4}$ – $10^{-3}$  of the resting fluorescent intensity (e.g., Figs. 2B, 7, and 8), the imaging device needs to have high saturation intensity, i.e., a well size of 100 million photons. In addition, an effective dynamic range of 17–19 bits is needed to digitize a  $10^{-4}$  signal. Ordinary CCD/CMOS cameras with a well size of 1–10 million photons and 10–14 bits of dynamic range will not be able to record the small signals shown in Figs. 2B, 7, and 8. Diode arrays offer an exceptional effective dynamic range by a parallel amplification design, i.e., each detector (pixel) has a dedicated two-stage amplifier (Cohen and Leshner 1986; for circuit diagram and additional information see Wu and Cohen 1993 and Jin et al. 2002.). Using the measurement of Fig. 2B as an example, the resting light intensity was  $\sim 1$  V at the output of the first stage. The signal, at  $\sim 10^{-3}$  of the resting light intensity, therefore

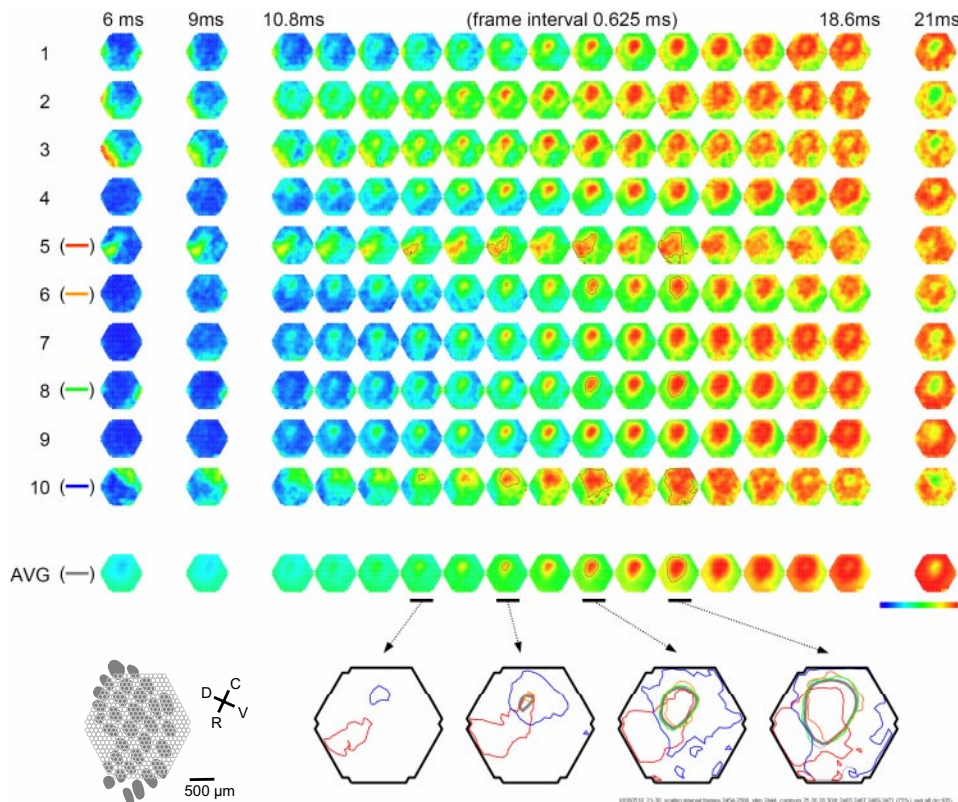


FIG. 9. Trial-to-trial variations in barrel cortex. *Image rows 1–10*: 10 consecutive trials with identical whisker deflection. *Bottom images (AVG)* are averaged from 105 trials from the same animal. *Bottom row left*: schematic diagram of barrel pattern and imaging field. *Bottom row right*: isochromatic contour lines were superimposed from trials 5 (red), 6 (orange), 8 (green), and 10 (blue), along with contour lines from averaged data (gray).

produced a change of  $\sim 1$  mV riding atop this resting 1 V. With a dedicated second stage amplifier for each pixel, the DC component (resting light intensity) can be easily removed by an analog circuit. After removing the DC component, the 1-mV signal is amplified 500 times to 500 mV. This signal is digitized with an A/D converter of 12 bits at a range of  $\pm 10$  V, resulting in the 500-mV signal being represented by  $\sim 8$  bits. Such high dynamic range is essential for the overall sensitivity of optical recordings (Figs. 2B, 7, and 8). The dark noise of the photodiode array is very small compared with shot noise ( $< 1/10$ ), and therefore instrumentation noise can be ignored. In the measurements of this report, we have achieved a signal-to-noise ratio of  $\sim 5$  from each single detector ( $0.016 \text{ mm}^2$ , with total 464 detectors in an area of 4 mm in diameter) at 1,600 frames/s (Fig. 7).

#### *Spatiotemporal resolution*

Spatial and temporal resolutions are closely linked and limited by shot noise. Higher spatiotemporal resolution leads to lower photon flux because of the smaller volume of tissue under each detector and because of the shorter sampling time. Lower photon flux has higher proportional shot noise and therefore lower signal-to-noise ratio. Increasing illumination intensity may further increase spatiotemporal resolution; however, phototoxicity might become a concern. Although RH1691 does not show toxicity under moderate light (Petersen et al. 2003a; Slovín et al. 2002), our illumination intensity was higher than previous reports, and we did observe rapid signal decline (Fig. 6). To address the concern of phototoxicity, results from later recording trials should be compared with those from the beginning of the experiment for verification.

#### *Differences between local field potential signal and VSD signal*

Figure 2 shows that VSD and local field potential recordings show good event-to-event correlation but a poor overall correlation. We speculate that the poor correlation in the waveforms was caused by the difference in origin of the two signals. The VSD signals originate from superficial cortical layers as indicated by the staining profile (Fig. 3). Local field potential signals, on the other hand, derive from local current flow, and therefore may contain volume-conducted signal from deeper cortical layers or strong subcortical sources. Although quantitative analyses of the correlation between the VSD and local field potential signals are beyond the scope of this paper, we believe that the issue may be important for understanding how subcortical input manifests in the cortex. Our data suggest a useful method for separating superficial and deep cortical components in local field potential recordings.

#### *Visualizing propagating waves*

Many cortical activities are spatiotemporally organized as propagating waves (“traveling waves”; Ermentrout and Kleinfeld 2001). Propagating waves have been extensively examined in cortical slices (Albowitz and Kuhnt 1995; Bao and Wu 2003; Chagnac-Amitai and Connors 1989; Chervin et al. 1988; Demir et al. 1998; Fleidervish et al. 1998; Golomb and Amitai

1997; Huang et al. 2004; Miyakawa et al. 2003; Tanifuji et al. 1994; Tsau et al. 1998; Wadman and Gutnick 1993; Wu et al. 1999, 2001). Because the velocity and direction of propagation are highly dynamic, the ability to record from single trials is essential for studying wave propagation. Before introduction of the blue dyes, sensory-evoked waves could only be imaged in the brain of turtle (Lam et al. 2000, 2003; Precht et al. 1997; Senseman and Robbins 1999, 2002), salamander (Cinelli et al. 1995), and invertebrate (Delaney et al. 1994; Kleinfeld et al. 1994), where heartbeat is not present or can be paused with cooling. The pulsation artifact of red dye RH795 had an amplitude of 0.5–1% of resting light intensity, similar to that of epileptiform spikes induced by bicuculline (Fig. 4A), and  $\sim 10$  times larger than the sensory-evoked cortical activity (London et al. 1989). With the use of blue dyes, pulsation artifact is greatly reduced and sensory evoked waves can be seen in mammalian cortex (Derdikman et al. 2003; Ferezou et al. 2006; Petersen et al. 2003a,b).

#### *Pulsation artifact*

RH1691 shows virtually no hemoglobin absorption artifact (Figs. 4 and 5; Ferezou et al. 2006; Shoham et al. 1999), but pulsating movement artifact may still be large. Imaging with the dura mater intact increased stability, and ECG-triggered subtraction further removed residual movement artifact time-locked to the heartbeat (Fig. 5). In a 10-s recording trial, there are  $\sim 50$  heartbeats; therefore signals that are not time-locked to the ECG would be distorted by  $< 2\%$ . The results are similar to other advanced mathematical methods, such as independent component analysis and advanced frequency domain analysis (Mitra and Pesaran 1999; Pesaran et al. 2005; Reidl et al. 2007).

#### *Limitations of the method*

The main limitation of VSD imaging methods is that the signals are from the superficial layers of the cortex (Fig. 3). Further improvements in this regard will await newer staining methods or bioengineered VSDs. Our transdural staining and imaging is also limited in species, because carnivores and primates have thicker and less translucent dura. The Grinvald group and others have described artificial dural implants (Chen et al. 2002; Slovín et al. 2002), which may provide sufficient mechanical stability in those species to obtain a large number of stable single trial recordings. Another limitation is that VSD recording is not a preferred way to measure DC signal. This is mainly because the DC component in VSD signal is contaminated by dye bleaching. In the process of making pseudocolor maps in this report, the signals were digitally filtered above 2–3 Hz to emphasize the propagating wave front. However, our cut-off at low frequency can be as low as 0.06 Hz, which is low enough to capture all low frequency components reflected in conventional EEG signals. The third limitation to this method is the use of anesthetized and firmly fixed animals. Elimination of motion is necessary for high-sensitivity recordings. This could perhaps be alleviated by novel and humane awake fixation methods or by optical-fiber based tether method (Ferezou et al. 2006).

In conclusion, the methods described in this report offer high signal-to-noise ratio recordings for a number of applications,

such as the study of trial-to-trial variability of sensory evoked waves, interaction between evoked and spontaneous activity, event-related activity in higher cortical areas, the interactions between individual neurons and local population, and the complex dynamics of epileptic activity.

## ACKNOWLEDGMENTS

We thank Drs. Shigeru Tanaka, Lawrence Cohen, and Amiram Grinvald for helpful comments.

Present address of M. T. Lippert: Leibniz-Institut für Neurobiologie; 39118 Magdeburg; Germany.

## GRANTS

This study was supported by National Institute of Neurological Disorders and Stroke Grant R01 NS-036447 to J.-Y. Wu and fellowships from the German National Academic Foundation to M. T. Lippert and the Epilepsy Foundation to X. Huang.

## REFERENCES

- Albowitz B, Kuhnt U.** Epileptiform activity in the guinea-pig neocortical slice spreads preferentially along supragranular layers—recordings with voltage-sensitive dyes. *Eur J Neurosci* 7: 1273–1284, 1995.
- Arieli A, Shoham D, Hildesheim R, Grinvald A.** Coherent spatiotemporal patterns of ongoing activity revealed by real-time optical imaging coupled with single-unit recording in the cat visual cortex. *J Neurophysiol* 73: 2072–2093, 1995.
- Bao W, Wu JY.** Propagating wave and irregular dynamics: spatiotemporal patterns of cholinergic theta oscillations in neocortex in vitro. *J Neurophysiol* 90: 333–341, 2003.
- Chagnac-Amitai Y, Connors BW.** Horizontal spread of synchronized activity in neocortex and its control by GABA-mediated inhibition. *J Neurophysiol* 61: 747–758, 1989.
- Chen LM, Heider B, Williams GV, Healy FL, Ramsden BM, Roe AW.** A chamber and artificial dura method for long-term optical imaging in the monkey. *J Neurosci Methods* 113: 41–49, 2002.
- Chervin RD, Pierce PA, Connors BW.** Periodicity and directionality in the propagation of epileptiform discharges across neocortex. *J Neurophysiol* 60: 1695–1713, 1988.
- Cinelli AR, Neff SR, Kauer JS.** Salamander olfactory bulb neuronal activity observed by video rate, voltage-sensitive dye imaging. I. Characterization of the recording system. *J Neurophysiol* 73: 2017–2032, 1995.
- Cohen LB, Keynes RD, Hille B.** Light scattering and birefringence changes during nerve activity. *Nature* 218: 438–441, 1968.
- Cohen LB, Leshner S.** Optical monitoring of membrane potential: methods of multisite optical measurement. *Soc Gen Physiol Ser* 40: 71–99, 1986.
- Delaney KR, Gelperin A, Fee MS, Flores JA, Gervais R, Tank DW, Kleinfeld D.** Waves and stimulus-modulated dynamics in an oscillating olfactory network. *Proc Natl Acad Sci USA* 91: 669–673, 1994.
- Demir R, Haberly LB, Jackson MB.** Voltage imaging of epileptiform activity in slices from rat piriform cortex: onset and propagation. *J Neurophysiol* 80: 2727–2742, 1998.
- Derdikman D, Hildesheim R, Ahissar E, Arieli A, Grinvald A.** Imaging spatiotemporal dynamics of surround inhibition in the barrels somatosensory cortex. *J Neurosci* 23: 3100–3105, 2003.
- Ermentrout GB, Kleinfeld D.** Traveling electrical waves in cortex: insights from phase dynamics and speculation on a computational role. *Neuron* 29: 33–44, 2001.
- Ferezou I, Bolea S, Petersen CC.** Visualizing the cortical representation of whisker touch: voltage-sensitive dye imaging in freely moving mice. *Neuron* 50: 617–629, 2006.
- Fleiderovich IA, Binshtok AM, Gutnick MJ.** Functionally distinct NMDA receptors mediate horizontal connectivity within layer 4 of mouse barrel cortex. *Neuron* 21: 1055–1065, 1998.
- Golomb D, Amitai Y.** Propagating neuronal discharges in neocortical slices: computational and experimental study. *J Neurophysiol* 78: 1199–1211, 1997.
- Grinvald A, Hildesheim R.** VSDI: a new era in functional imaging of cortical dynamics. *Nat Rev Neurosci* 5: 874–885, 2004.
- Grinvald A, Manker A, Segal M.** Visualization of the spread of electrical activity in rat hippocampal slices by voltage-sensitive optical probes. *J Physiol* 333: 269–291, 1982.
- Gutnick MJ, Connors BW, Prince DA.** Mechanisms of neocortical epileptogenesis in vitro. *J Neurophysiol* 48: 1321–1335, 1982.
- Huang X, Troy WC, Yang Q, Ma H, Laing CR, Schiff SJ, Wu JY.** Spiral waves in disinhibited mammalian neocortex. *J Neurosci* 24: 9897–9902, 2004.
- Jin W, Zhang RJ, Wu JY.** Voltage-sensitive dye imaging of population neuronal activity in cortical tissue. *J Neurosci Methods* 115: 13–27, 2002.
- Kleinfeld D, Delaney KR.** Distributed representation of vibrissa movement in the upper layers of somatosensory cortex revealed with voltage-sensitive dyes. *J Comp Neurol* 375: 89–108, 1996.
- Kleinfeld D, Delaney KR, Fee MS, Flores JA, Tank DW, Gelperin A.** Dynamics of propagating waves in the olfactory network of a terrestrial mollusk: an electrical and optical study. *J Neurophysiol* 72: 1402–1419, 1994.
- Lam YW, Cohen LB, Wachowiak M, Zochowski MR.** Odors elicit three different oscillations in the turtle olfactory bulb. *J Neurosci* 20: 749–762, 2000.
- Lam YW, Cohen LB, Zochowski MR.** Odorant specificity of three oscillations and the DC signal in the turtle olfactory bulb. *Eur J Neurosci* 17: 436–446, 2003.
- London JA, Cohen LB, Wu JY.** Optical recordings of the cortical response to whisker stimulation before and after the addition of an epileptogenic agent. *J Neurosci* 9: 2182–2190, 1989.
- Ma HT, Wu CH, Wu JY.** Initiation of spontaneous epileptiform events in the rat neocortex in vivo. *J Neurophysiol* 91: 934–945, 2004.
- Mitra PP, Pesaran B.** Analysis of dynamic brain imaging data. *Biophys J* 76: 691–708, 1999.
- Miyakawa N, Yazawa I, Sasaki S, Momose-Sato Y, Sato K.** Optical analysis of acute spontaneous epileptiform discharges in the in vivo rat cerebral cortex. *Neuroimage* 18: 622–632, 2003.
- Momose-Sato Y, Sato K, Arai Y, Yazawa I, Mochida H, Kamino K.** Evaluation of voltage-sensitive dyes for long-term recording of neural activity in the hippocampus. *J Membr Biol* 172: 145–157, 1999.
- Pesaran B, Sornborger AT, Nishimura N, Kleinfeld D, Mitra PP.** Analysis of dynamic optical imaging data. In: *Imaging in Neuroscience and Development: A Laboratory Manual*, edited by Yuste R, Konnerth A. Cold Spring Harbor, New York: Cold Spring Harbor Laboratory Press, 2005, p. 815–826.
- Petersen CC, Grinvald A, Sakmann B.** Spatiotemporal dynamics of sensory responses in layer 2/3 of rat barrel cortex measured in vivo by voltage-sensitive dye imaging combined with whole-cell voltage recordings and neuron reconstructions. *J Neurosci* 23: 1298–1309, 2003a.
- Petersen CC, Hahn TT, Mehta M, Grinvald A, Sakmann B.** Interaction of sensory responses with spontaneous depolarization in layer 2/3 barrel cortex. *Proc Natl Acad Sci USA* 100: 13638–13643, 2003b.
- Prechtel JC, Cohen LB, Pesaran B, Mitra PP, Kleinfeld D.** Visual stimuli induce waves of electrical activity in turtle cortex. *Proc Natl Acad Sci USA* 94: 7621–7626, 1997.
- Regan MJ, Eger EI.** Effect of hypothermia in dogs on anesthetizing and apneic doses of inhalation agents. Determination of the anesthetic index (Apnea/MAC). *Anesthesiology* 28: 689–700, 1967.
- Reidl J, Starke J, Omer DB, Grinvald A, Spors H.** Independent component analysis of high-resolution imaging data identifies distinct functional domains. *Neuroimage* 34: 94–108, 2007.
- Ross WN, Salzberg BM, Cohen LB, Grinvald A, Davila HV, Waggoner AS, Wang CH.** Changes in absorption, fluorescence, dichroism, and birefringence in stained giant axons: optical measurement of membrane potential. *J Membr Biol* 33: 141–183, 1977.
- Senseman DM, Robbins KA.** Modal behavior of cortical neural networks during visual processing. *J Neurosci* 19: RC3, 1999.
- Senseman DM, Robbins KA.** High-speed VSD imaging of visually evoked cortical waves: decomposition into intra- and intercortical wave motions. *J Neurophysiol* 87: 1499–1514, 2002.
- Shoham D, Glaser DE, Arieli A, Kenet T, Wijnbergen C, Toledo Y, Hildesheim R, Grinvald A.** Imaging cortical dynamics at high spatial and temporal resolution with novel blue voltage-sensitive dyes. *Neuron* 24: 791–802, 1999.
- Slovin H, Arieli A, Hildesheim R, Grinvald A.** Long-term voltage-sensitive dye imaging reveals cortical dynamics in behaving monkeys. *J Neurophysiol* 88: 3421–3438, 2002.
- Spors H, Grinvald A.** Spatio-temporal dynamics of odor representations in the mammalian olfactory bulb. *Neuron* 34: 301–315, 2002.

- Tanifuji M, Sugiyama T, Murase K.** Horizontal propagation of excitation in rat visual cortical slices revealed by optical imaging. *Science* 266: 1057–1059, 1994.
- Tasaki I, Watanabe A, Sandlin R, Carnay L.** Changes in fluorescence, turbidity, and birefringence associated with nerve excitation. *Proc Natl Acad Sci USA* 61: 883–888, 1968.
- Tsau Y, Guan L, Wu JY.** Initiation of spontaneous epileptiform activity in the neocortical slice. *J Neurophysiol* 80: 978–982, 1998.
- Wadman WJ, Gutnick MJ.** Non-uniform propagation of epileptiform discharge in brain slices of rat neocortex. *Neuroscience* 52: 255–262, 1993.
- Wu JY, Cohen LB.** Fast multisite optical measurement of membrane potential. In: *Fluorescent and Luminescent Probes of Biological Activity*, edited by Mason WT. San Diego, CA: Academic Press, 1993, p. 389–404.
- Wu JY, Guan L, Bai L, Yang Q.** Spatiotemporal properties of an evoked population activity in rat sensory cortical slices. *J Neurophysiol* 86: 2461–2474, 2001.
- Wu JY, Guan L, Tsau Y.** Propagating activation during oscillations and evoked responses in neocortical slices. *J Neurosci* 19: 5005–5015, 1999.